Journal Homepage: https://dergipark.org.tr/tr/pub/isibted

Isı Bilimi ve Tekniği Dergisi

Archive: https://tibtd.org.tr/dergi

Investigation Of Increasing Process Gas Cooling Performance By Improving Ammonia Oxidation Reactor Heat Exchangers

Fadime Menekşe İKBAL [1], Oğuzhan ERBAŞ [1,*]

[1] Kütahya Dumlupınar Üniversitesi, Mühendislik Fakültesi, Makine Mühendisliği Bölümü, 43100, Kütahya, Türkiye

A R T I C L E   I N F O

2025, vol. 45, no.1, pp. 97-110
©2025 TIBTD Online.
doi: 10.47480/isibted.1566904

Research Article
Received: 14 October 2024
Accepted: 16 December 2024

* *Corresponding Author*
e-mail: oguzhan.erbas@dpu.edu.tr

Keywords:
Process Gas Cooling
Oxidation Reactor
Heat Exchanger
CFD Analysis

ORCID Numbers in author order:
0000-0002-5665-7306
0000-0001-9424-4273

A B S T R A C T

This study aims to increase the cooling performance of NO_x gas by improving the heat exchangers of an industrial-type ammonia oxidation reactor with a diameter of 3.8 m and a height of 6.5 m in a nitric acid production plant with a capacity of 610 tons/day. The reactor produces 100% HNO_3, 56% diluted nitric acid, and 33 tons/hour of superheated steam. To this end, the parametric analysis study, in which the horizontal and vertical distance between the exchanger tubes, the pipe diameters, and the distance between the exchanger packages (pre-evaporator, superheater, evaporator, economizer) were used separately, was carried out with the help of Ansys Fluent program and the flow properties and performance values were examined. The best cooling performance (for the inner part of the ammonia oxidation reactor) resulted from different parametric studies; there was a study in which the process gas temperature was obtained at 270.51^{0}C with a 56 mm horizontal distance between the heat exchanger tubes (a). Thus, a 9.1% decrease in the actual gas outlet temperature of the operating reactor was achieved. In other parametric studies, the lowest process gas temperatures are; it was found to be 323.20^{0}C for the distance between heat exchanger packages (L), 318.42 ^{0}C for the vertical distance between heat exchanger tubes (b), and 296.67 ^{0}C for the heat exchanger tube diameter (D). In addition, when the CFD simulation results, which provide the best cooling performance, are compared with actual operating data (SCADA online data), In the ammonia oxidation reactor, the fluid outlet temperature increased by 8.2% in the economizer, 9.7% in the evaporator and 4.3% in the superheater.

Amonyak Oksidasyon Reaktörü Isı Değiştiricilerinin İyileştirilerek Proses Gaz Soğutma Performansının Artırılmasının Araştırılması

M A K A L E   B İ L G İ S İ

Anahtar Kelimeler:
Proses Gaz Soğutma
Oksidasyon Reaktörü
Isı Değiştirici
CFD Analizi

Ö Z E T

Bu çalışmada, 610 ton/gün kapasiteli bir nitrik asit üretim tesisindeki 3,8 m çapında ve 6,5 m yüksekliğindeki endüstriyel tip amonyak oksidasyon reaktörünün ısı değiştiricilerini iyileştirerek, NO_x gazının soğutma performansının artırılması amaçlanmıştır. Reaktör, % 100 HNO_3, %56 seyreltilmiş nitrik asit ve 33 ton/saat aşırı ısıtılmış buhar üretmektedir. Bu amaçla, eşanjör boruları arasındaki yatay ve düşey mesafe, boru çapları ve eşanjör paketleri (ön buharlaştırıcı, aşırı ısıtıcı, buharlaştırıcı, ekonomizer) arasındaki mesafenin ayrı ayrı kullanıldığı parametrik analiz çalışması, Ansys Fluent programı yardımıyla yapılmış ve akış özellikleri ile performans değerleri incelenmiştir. En iyi soğutma performansı farklı parametrik çalışmalar sonucunda; ısı değiştirici boruları arasında yatay olarak 56 mm mesafede proses gazı sıcaklığının 270,5 ^{0}C elde edildiği çalışma ile sağlanmıştır. Böylece, reaktörün gaz çıkış sıcaklığında % 9,1'lik bir azalma sağlanmıştır. Diğer parametrik çalışmalarda ise en düşük proses gazı sıcaklıkları; ısı değiştirici paketleri arasındaki mesafe (L) için 323,2 ^{0}C, ısı değiştirici boruları arasındaki dikey mesafe (b) için 318,4 ^{0}C ve ısı değiştirici boru çapı (D) için 296,6 ^{0}C olarak bulunmuştur. Ayrıca, en iyi soğutma performansını sağlayan CFD simülasyon sonuçları, gerçek işletme verileriyle (SCADA verileri ile) karşılaştırıldığında; amonyak oksidasyon reaktöründe soğutucu akışkan çıkış sıcaklığı ekonomizerde %8,2, buharlaştırıcıda %9,7 ve süperheater'da %4,3 artmıştır.

NOMENCLATURE

SCADA	Supervisory control and data acquisition	AOR	Ammonia oxidation reactor
CFD	Computational fluid dynamics	PGC	Process gas cooler
Pt-Rh	Platinum radium	HEP	Heat Exchanger Packages
LMN	La Mont nozzles	D	Heat exchanger tube diameter
ρ	Gas phase density (kg/m^3)	L	Distance between heat exchanger packages
C_p	Gas phase heat capacity (J/mol.k)	b_t	Vertical distance between heat exchanger tubes
K_h	Heat transfer coefficient (W/m^2.K)	TNT	Trinitrotoluene

INTRODUCTION

Energy efficiency has an essential place in the policies of most developed countries. The importance of energy efficiency as a policy goal depends on its benefits for trade, industrial competitiveness, and energy security. "Nitric acid production," one of the essential inorganic acids, also includes a series of energy conversion processes. It neutralizes nitric acid with ammonia, making ammonium nitrate the most critical component of worldwide mineral fertilizers. It provides plants and ornamental plants with the nitrogen they need to grow in high, easily digestible doses (Heck et al., 1982; Juangsa et al., 2019). Additionally, HNO_3 can be used for soil acidification in horticulture. In the chemical industry, nitric acid is primarily a precursor to organic nitrogen compounds such as nitrobenzenes. Combined with aromatic compounds, it gives substances used to make explosives, such as TNT and nitroglycerin. Another critical application is rocket fuel. For this purpose, a mixture of HNO_3, dinitrogen tetroxide, and hydrogen peroxide, also known as red-fuming nitric acid, is prepared (Hernández et al., 2021). Its use in the space industry depends on efficiently storing raw materials. The potential of nitric acid for plastic production is also notable. The oxidation it initiates produces adipic acid, also used to make synthetic fibers such as nylon (Neumann et al., 2024; Sadykov et al., 2020). In the production of nitric acid, first ammonia is oxidized to obtain nitric oxide (nitrogen monoxide, NO); then NO is further oxidized to NO_2 (nitrogen dioxide). In the last stage, NO_2 gas is absorbed with water to obtain Nitric Acid (HNO_3). This process is called the “Ostwald Process”. The ammonia oxidation reactor is the most crucial step in this process flow diagram. The filtered air is heated after being pressurized. After evaporation with heated air, the filtered NH_3 is mixed and fed to the reactor containing a platinum/rhodium alloy catalyst. A reversible and exothermic reaction occurs between NH_3 and oxygen in the reactor, releasing nitrogen oxides (NO_x) (Dong et al., 2023; Chatterjee et al., 2008). This heat released from the oxidation reaction can be recovered using heat exchangers, and the system's energy efficiency can be increased. Heat is usually used in other processes to save energy. In addition, the temperature of the NO_x gases affects the reaction's progress and the catalyst's efficiency. If the reactor temperature is too high, unwanted side reactions and by-products can occur. In addition, very high temperatures can lead to catalyst deterioration or inefficient operation. Therefore, controlled cooling of the temperature of the NO_x gases is essential for the efficiency of the reaction. NO_x gases can become more stable at very high temperatures, making subsequent purification and reaction stages difficult. Cooling helps to keep the NO_x in a more stable and processable form. In addition, in some cases, NO_x gases, after cooling, can be more easily processed or separated by other reactions. As a result, controlled cooling of the temperature of the NO_x gases is a critical step in reaction efficiency, energy management, and chemical processing (Abbasfard et al., 2014; Mewada et al., 2015).

When temperatures are low or the catalyst is not working, the chemical reaction can slow down or partially slow down (Salam et al., 2016). The entrance region of the reactor is a critical point where the chemical reaction begins. Optimizing this region's temperature, pressure, and flow rate is necessary to initiate and continue the reaction (Amirsadat et al., 2024). Burner head geometry and design directly affect the mixing and distribution of gases. If a homogeneous gas distribution is not achieved, temperature and reactant distribution irregularities may occur on the catalyst, reducing efficiency (Nascimento et al., 2024; Holma et al., 1979). When literature studies on ammonia oxidation reactors examine production and process efficiency, they generally focus on the reactor inlet region and burner head geometry design, flow pattern and catalyst structure, and gauze platinum losses. Moszowski et al. (2019) analyzed the gas velocity distribution in an ammonia oxidation reactor. Three different design arrangements of the burner head (reactor header - inlet section) were examined to verify the effects of the liquid flow rate entering the catalysts. This paper analyzes how different burner head designs, such as screens made of perforated plates, cone diffusers, and guide vanes, affect the uniformity of the gas flow through the catalyst gauze in a nitric acid plant reactor. It was found that the accurately selected perforated plate and the conical diffuser solved the problem of ensuring the proper flow of gas on ammonia oxidation catalysts and catalysts for nitrous oxide decomposition (Kraehnert et al., 2008). Using CFD analysis, Abbasfard et al. (2012) simulated the flow inside the industrial ammonia oxidation reactor. The simulation results clearly showed the poor flow distribution inside the reactor. The direct effect of such a failure can be seen in the uneven (non-homogeneous) temperature distribution around the reactor shell. Thermography experiments were also conducted to support this claim and revealed the fact that the left side of the reactor experienced higher temperatures. The contour plots also showed some stagnant and swirling regions before or after the distribution of the reactor due to the poor flow distribution. Wiser examined a modeling approach in which a mechanistic model of ammonia oxidation on platinum (catalyst site), previously published by Kraehnert and Baerns, was implemented in a CFD simulation using a rate-matching approach. The effect of geometry on the process performance of the catalytic gauze was improved by using the knowledge gained through CFD simulations in which detailed kinetics were included(Wiser et al., 2020). Chatterjee et al. (2008) attempted to understand the rate-controlling step for the ammonia oxidation process, mass transfer and chemical reaction rates for nitrogen oxide absorption, and the combined effects of various equilibria in optimizing heat recovery from a product stream in the ammonia oxidation reactor. Also, the impact of geometrical parameters, excess air, degree of absorption, product acid concentration, temperature, and pressure for the absorption column were analyzed to optimize the nitric acid plant. They found that the optimum operating pressure increases as the restriction on the NO_x outlet concentration increases. Grande et al. (2018) aimed to convert the homogeneous noncatalytic nitric oxide oxidation into a faster catalytic step. With this conversion, the energy recovery of nitric acid production is expected to increase by up to 10%. For this purpose, a platinum-catalyzed process on alumina was investigated. They found that since the reaction also proceeds in the gas phase, it is essential to limit the contact time of NO and O_2 before the catalyst and, for the same reason, the outlet flow length between the reactor and the analyzer should be reduced as much as possible (to limit the interaction of unconverted NO and O_2) (Grande et al., 2018). Elsayed et al. (2023) present a model for an industrial catalytic ammonia oxidation reactor using a Pt/Rh catalyst gauze for nitric oxide production in a nitric acid plant. They utilized two fundamental models to perform mass and energy balance analyses integrated with MATLAB 2017. The first model focused on mass balance, predicting the variations in concentrations of nitrogen (N), nitric oxide (NO), and oxygen (O) along the catalyst bed of the reactor, which has a diameter of 4.8 meters and a height of 1 meter. The second model addressed energy balance, predicting temperature variations within the same catalyst bed. In the mass balance model, the deviation for nitric oxide concentration did not exceed 6.2%. For the energy balance model, the deviation was only 0.4%. These mathematical models accurately predicted operational values with minimal deviation(Elsayed et al., 2023; Kayapinar et al., 2024). Scheuer et al. (2011) modeled a high-efficiency single-channel monolith reactor for ammonia oxidation. A mechanistic model was used to oxidize ammonia on platinum, and all internal and external mass transfer effects were included. Model efficiencies were derived from using previously calculated solutions of the mass balance equations (Scheuer et al., 2011; Ardy et al., 2021).

In high-capacity chemical processes such as nitric acid production, the gas flow dynamics, temperature profiles, and heat transfer mechanisms of these reactors directly affect the overall performance and sustainability of the system. The main objective of this study is to investigate the thermal performance of an ammonia oxidation reactor used in a nitric acid production facility with a capacity of 610 tons/day. The study aims to optimize the heat transfer between the reactor and the cooling exchangers. In particular, the effects of geometric parameters such as horizontal and vertical distance between the pipes on the temperature profile of the process gas are analyzed. The reactors in the nitric acid production facility consist of two parts: the catalyst, where catalytic combustion occurs, and the waste heat boiler (where the heat exchanger packages are located), where heat transfer occurs. It is seen that the studies in the literature mainly focus on the inlet part of the ammonia oxidation reactor (air + NH_3) gas mixing reaction (gas flow properties) and the geometry of this region. This study focuses on determining energy-intensive processes in the nitric acid production plant, significantly improving the NOx gas cooling performance by enhancing the ammonia oxidation reactor heat exchangers. A parametric analysis was performed to achieve this goal, and flow characteristics and performance values were examined using the Ansys Fluent program. Especially in such critical processes, heat exchangers are essential in increasing energy efficiency and optimizing system performance. Therefore, it was decided to examine the following factors.

- Fluid Inlet-Outlet Points and Temperature Distribution: The temperature distribution at the inlet and outlet points directly affects the heat transfer efficiency. Optimizing the temperature differences increases the efficiency of heat exchangers.
- Distance Between Tubes: The horizontal and vertical distance between the tubes affects the interaction of the fluids with each other and heat transfer. Optimizing this distance can increase the cooling performance of the gas and thus increase the system's overall efficiency.
- Tube Diameter: The tube diameter affects the flow rate and heat transfer surface. Choosing the correct diameter allows the fluid to be cooled more effectively and minimizes energy losses. Examining these elements regarding system efficiency is necessary to reduce energy consumption, lower operating costs, and minimize environmental impacts. In addition, simulation techniques such as CFD (Computational Fluid Dynamics) allow detailed analysis of these parameters to obtain more effective designs. In line with these hypotheses, the effects of critical parameters of the reactor system design on thermal performance were simulated by the computational fluid dynamics (CFD) method in the study, and the results were compared with actual operating data (SCADA). The study aims to develop design recommendations that can optimize the system performance and evaluate these findings regarding economic and environmental sustainability.

STRUCTURE AND PROPERTIES OF THE ANALYZED AMMONIA OXIDATION REACTOR

The oxidation reactor and heat exchanger pipes within the nitric acid production facility, which were analyzed to increase efficiency, are shown (Figure 1).

Figure 1. Analyzed Industrial Ammonia Oxidation Reactor and Heat Exchanger Pipes (Process Gas Coolers Oper. and Maint. Man., 2024)

This reactor is a cylindrical body with a diameter of 3.8 m and a length of 6.5 m. It contains a catalyst layer made of platinum-rhodium. Ammonia is gasified with water in the ammonia gasifier and comes to the combustion unit. The air required for the combustion of ammonia is cleaned in the oil filter and sucked from the atmosphere through the turbo compressor and comes to the combustion unit reactor. Then, ammonia and air at the same temperature are mixed in the mixer section. A chemical reaction in the platinum-radium catalyst burns this mixture of ammonia and air. Filter tubes made of porous ceramic material are placed at the bottom. The gas mixture is cleaned by passing through porous tubes. Then, by passing through the catalyst layer, ammonia turns into NO. An exothermic reaction occurs between ammonia and oxygen in the gas phase. The NO_x gases released from this catalyst come to the waste heat boiler and leave the reactor, leaving their heat in the coils. Regarding the system's overall efficiency, it aims to cool NO_x gases as much as possible in this part of the process (Hannevold et al., 2005; Hung et al., 2008). This ammonia oxidation reactor consists of two main parts. The first is the combustion unit part (chemical reaction), and the second is the waste heat boiler part, which produces steam. Combustion unit: The roof part, where the catalyst is located, is where the chemical reaction occurs. The ammonia-air mixture is burned to form nitrogen monoxide and water vapor. This part is also called the incinerator. This is the first part of the facility. Reactors that contain a gauze catalyst are used in the production of HCN from CH_4, NH_3, and O_2 (known as the Russow process), as well as in the creation of nitrogen oxides during the production of nitric acid (known as the Ostwald process). The Ostwald process occurs here at the catalyst (Fajardo et al., 2018; Elsayed et al., 2023). Chemical reaction on catalysts occurs at high temperatures (860 ~ 900^{o}C). Approximately 11 % ammonia reacts with 89 % air in the chemical reaction. Figure 2. shows the main steps of the Ostwald process.

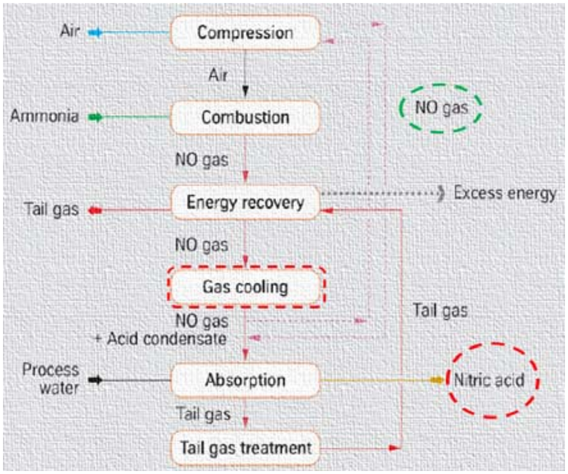

Figure 2. Block diagram of the Ostwald process (Grande et al., 2018)

The only catalyst used industrially in the process is the platinum-radium catalyst, which contains 5 % to 10 % radium and is called platinum. This catalyst, that is, platinum radium (Pt-Rh) catalyst, contains 95 % platinum and 5 % radium. It is in the form of a fine mesh. The reaction occurs in a very short time. Conversion efficiency varies between 90-96% depending on reaction conditions. Oxygen atoms are absorbed on the platinum surface. The reaction takes place between oxygen atoms and ammonia molecules on the surface. Then, the ammonia molecule turns into NO. The system uses two 320 m^3/h capacity circulation pumps. The pumps have an inlet pressure of 44 bar and an outlet pressure of 47.9 bar. The cooling water circulating in the system is also a suitable, non-aggressive fluid that is not prone to deposit formation and does not contain suspended particles. The acceptable hardness value for this fluid in the system is 1.4 mmol/l, and the pH value is approximately between 7.5 and 9. Thanks to the nozzles inside the reactor, water is directed equally to the evaporator and cooling tubes, contributing to increased cooling performance. This prevents thermal stresses and equipment damage that may arise from temperature differences. The location and types of nozzles and their diameter characteristics are given in Table 1. The holes of different diameters used in La Mont nozzles (LMN) are optimized according to these different thermal loads. Larger holes provide higher water flow, while smaller holes provide lower flow. This ensures that each system section is cooled according to its requirements.

Table 1. Locations, Types, and Features of La Mont Nozzles (LMN) in Cooling Zones

Locations	Tube [mm]	pcs.	Ø [mm]	Locations	Tube [mm]	pcs.	Ø [mm]
Pre-evap. Layer $_{1,2}$	42.4 x 4	13	9	Evap. Layer $_{4,6}$	42.4 x 4	6	8
Pre-evap. Layer $_3$	42.4 x 4	3 1	9,5 10	Evap. Layer $_{7,8}$	42.4 x 4	4	7.5
Evap. Layer $_{1,2}$	2.4 x 4	6	8	Evap. Layer $_{9,10}$	42.4 x 4	3 1	7 10
Evap. Layer $_3$	42.4 x 4	2	8,5	Evap. Layer$_{11,12}$	42.4 x 4	2	8

Kinetic Mechanism of Ammonia Oxidation

Figure 3. shows the oxidation reaction mechanism with Pt-Rh catalyzed raschig rings (Il'chenko et al., 1975).

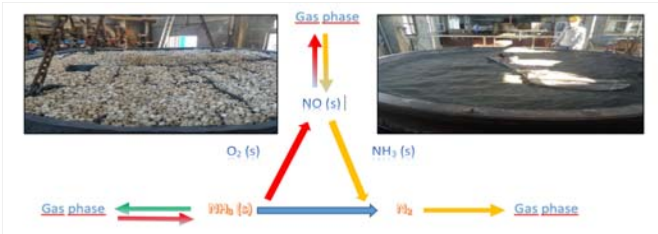

Figure 3. Mechanism of Oxidation Reaction with Pt-Rh Catalyzed Raschig Rings.

The kinetic mechanism of ammonia oxidation provides fundamental information for reactor design and chemical engineering in general. For these reasons, the kinetic mechanism of ammonia oxidation is essential for research and applications (Fila et al., 1994; Il'chenko et al., 1975). The reaction rate is controlled by the transfer of ammonia from the bulk gas to the platinum surface, depending on contact time and reaction mixture composition. Previous theories regarding ammonia oxidation on platinum presumed that transient compounds are formed. However, experiments indicate that the reactions of components on the catalyst surface involve no transient compounds. Pignet and Schmidt conducted a study on the selectivity of the oxidation of NH on Pt and the kinetics of oxidation on Pt-Rh and Pd. They conducted experiments in a low-pressure reactor connected to a mass spectrometer and suggested a simple series-parallel mechanism based on the concept by Fogel and Coworkers. Zhan et al. (2024) developed a kinetic model applicable to ammonia oxidation under high-pressure conditions. They validated it against the performance of other recently published kinetic models concerning various parameters related to ammonia oxidation and NO_x emission under high-pressure situations. The developed model was also validated with published experimental data collected under high-pressure conditions (Zhan et al., 2024; Chernyshev et al., 2001). The kinetic parameters in equations (1,2,3) and (4,5,6) were obtained from experimental data measured at low pressures, not exceeding 15 Pa. While the kinetic equations can be applied to calculate reactors operating at atmospheric or elevated pressures, it is essential to note that outer diffusion has a strong effect on the total reaction rates, leading to a substantial decrease in the concentrations of reactants on the catalyst surface. In industrial applications of the Pt-Rh catalyst under conventional conditions, the ratio of ammonia partial pressure in the gas phase to that at the catalyst surface is approximately 10-4 (Il'chenko et al., 1975). The following relations give the formation rates for NO and N_2 (Fila et al., 1994).

$$F_{NO} = \frac{2.209.10^{-11} exp\left(\frac{90\,791.6}{RT_S}\right) P_{NH_3} Po_2^{1/2}}{(£_{\mathrm{NOa}} + £_{\mathrm{NOb}})} \tag{1}$$

$$£_{\mathrm{NOa}} = \left(1 + 6.928.10^{-3} \exp\left(\frac{1\,840.93}{\mathrm{RT_S}}\right) \mathrm{Po}_2^{\frac{1}{2}}\right) \tag{2}$$

$$£_{\mathrm{NOb}} = \left(\left(1 + 1.2.10^{-5} exp\left(\frac{106.690.5}{RT_S}\right) Po_2^{1/2}\right) P_{NH_3}\right) \tag{3}$$

$$F_{N_2} = £_{N_{2a}} + £_{N_{2b}} \tag{4}$$

$$£_{N_{2a}} \frac{2.36.10^{-15} exp\left(\frac{108\,782.5}{RT_S}\right) P_{NH_3} P_{NO}}{\left(1 + 4.05.10^{-4} exp\left(\frac{45\,605}{RT_S}\right) PO_2 + 3.38.10^{-8} exp\left(\frac{87\,444}{RT_S}\right) P_{NH_3}\right)^{2}} \tag{5}$$

$$£_{N_{2b}} \frac{1.65.10^{-8} exp\left(\frac{-2.385}{RT_S}\right) P_{NH_3}}{\left(1 + 4.05.10^{-4} exp\left(\frac{45\,605}{RT_S}\right) PO_2 + 3.38.10^{-8} exp\left(\frac{87\,444}{RT_S}\right) P_{NH_3}\right)} \tag{6}$$

In industrial converters, total pressure hurts the NO yield due to the reaction between NH and NO in the gas phase. Wisc and Frech have examined the kinetics of this reaction. They derived an equation based on experiments where they monitored the total gas pressure in the apparatus over time due to reaction (Equations 7 and 8).

$$\frac{dP}{d_t} = k\, P_{NH_3} Po_{NO}^{-1/2} \tag{7}$$

k= 9.527 .109 exp (-229 018 / RT) (Pa ½ s-1) (8)

Equations (7-8) are mathematical equations representing the kinetics of NH oxidation on Pt gauzes in the temperature range from 600 to 1200 K. Consequently; these equations are used in industrial reactor modeling for the oxidation of NH_3 (Il'chenko et al., 1975).

Energy Balance Equation for an Industrial Ammonia Oxidation Reactor

In oxide studies, catalysts' activity is typically estimated by measuring their performance about the selectivity towards NO under industrial conditions. The lower the reaction ignition temperature, the higher the maximum NO selectivity and the lower the adequate activation energy and reaction order. This means that external diffusion limitations are more severe. Therefore, the selectivity towards NO is an essential measure of catalyst activity. This approach has been widely used in evaluating catalysts in practice (Kirova-Yordanova et al., 2011; Srinivasan et al., 1997). The catalytic ammonia oxidation process was simulated using a typical monolithic reactor model (Fila et al., 1994; Belghaieb et al., 2010), represented by the equation:

$$\rho C_P \frac{dT}{dt} = -v\, \rho C_P \frac{dT}{dz} - K_h(z) \frac{\alpha}{\varepsilon} (T - T^*) \tag{9}$$

The following variables are used in the equation: gas phase density (ρ) in kg/m^3 and gas phase heat capacity (C_p) in J/mol.k, gas phase temperature (T) in K, time (t) in s, linear velocity (v) in m/s, axial coordinate (z) in m, heat transfer coefficient (K_h) in W/m^2.K, specific surface area (a) in m^{-1}, void fraction (ε), and solid phase temperature (T^*) in K. The equation assumes one-dimensional steady-state conditions, constant solid phase temperature, and heat transfer coefficient (K_h). Therefore, the equation becomes as follows:

$$\frac{dT}{dt} = \frac{-K_h \alpha}{\varepsilon v \rho C_p} (T - T^*) \tag{10}$$

The value of ρ is calculated (Eq. 11) as the average density of the gas mixture at the inlet and outlet conditions of the catalyst bed.

$$\rho = \frac{PM_{mix}}{RT} \tag{11}$$

It is assumed that the C_p value is the average value between the C_p values of the gas mixture at the inlet and outlet conditions of the catalyst. This is based on previous research. The value of the heat transfer coefficient, K_h, is taken from the literature (Fila et al., 1994).

STUDY TO IMPROVE THE PROCESS GAS COOLING PERFORMANCE OF OXIDATION REACTOR HEAT EXCHANGERS

In the nitric acid production facility, the central heart of the process is the oxidation reactor. The main parameters affecting the system efficiency in the oxidation reactor are the NH_3 burning rate, platinum bottom temperature, and NO gas exit temperature. Reactor malfunction, maintenance, etc., and cut-out and stop times also affect system efficiency (Figure 4).

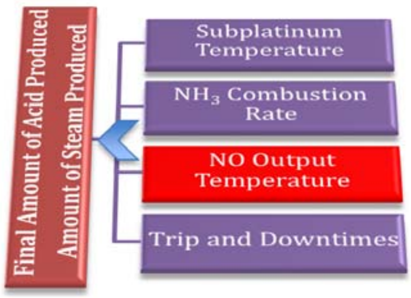

Figure 4. Main parameters affecting process efficiency

The effect of these parameters determines the final amounts of acid produced by the steam produced in the facility. The best option to increase system efficiency by improving these parameters is to reduce the NO gas outlet temperature as much as possible (Pfefferle et al., 1987; Moszowski et al., 2019). In the ammonia oxidation reactor, a mixture of approximately 11% ammonia + 89 % air is burned at approximately 870 °C on platinum-rhodium-palladium catalysts under 2.5–3.5 atu (kg/cm^2) pressure to obtain nitrogen oxide gas (NO). This gas obtained is the superheater, evaporator, pre-evaporator, and economizer, which also provide steam by transferring their heat to the circulating water. The more heat (cooling efficiency) extracted from NO gases in this process region increases, the more system efficiency will increase(Kraehnert et al., 2008; Schumacher et al., 2019). Exothermic reactions occurring within the reactor require thermal management. Heat exchangers help maintain process gases at appropriate temperatures (Bagheri et al., 2024; Juangsa et al., 2019). Controlling the temperature of process gases increases the efficiency of the reactor and prevents overheating of the reactor materials (Song et al., 2016; García-Ruiz et al., 2023). The reactor temperature must be constantly monitored and controlled. Automatic control systems ensure the temperature is kept within the desired range (Stagni et al., 2020). For this reason, the functions of gas cooling in the ammonia oxidation reactor are as follows: a design modeling study was carried out with CFD analysis for the pre-evaporator, superheater, evaporator, and economizer region. The numerical model used in the study is an exact scale model of the coils in the ammonia oxidation reactor.

The numerical model was drawn using the Solidworks program. The drawn model was transferred to the Ansys Workbench Space Claim program. It is known that an important parameter affecting the accuracy of the numerical solution is mesh independence (Colak, A. B. et al., 2024; Enger et al., 2018). For this reason, before moving on to numerical analysis, the drawn model was divided into different numbers of finite volumes for mesh independence studies. Figure 5. shows the created CAD/CAM model of the reactor. Mesh structures created with the Ansys Workbench Mesh program were also transferred to the Ansys Fluent program. Additionally, a mesh structure that does not affect the outcome of the solution for steady-state was determined.

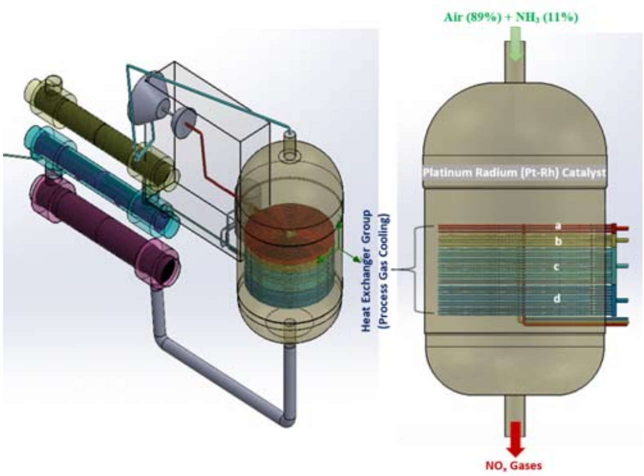

a: Pre-Evaporator b: Superheater c: Evaporator d: Economizer

Figure 5. Ammonia Oxidation Reactor (AOR) CAD/CAM Model

The mesh was created with the help of the Ansys Watertight geometry mesh program, as shown in Figure 6. Polyhedral elements were used in the border regions, and hex elements were used in the other areas. This study determined the most suitable mesh structure, turbulence model, and wall function for the problem studied. The number of meshes is closely related to the computer's RAM being studied. The maximum number of grids and elements was created according to the RAM capacity of the workstation where the calculations will be made.

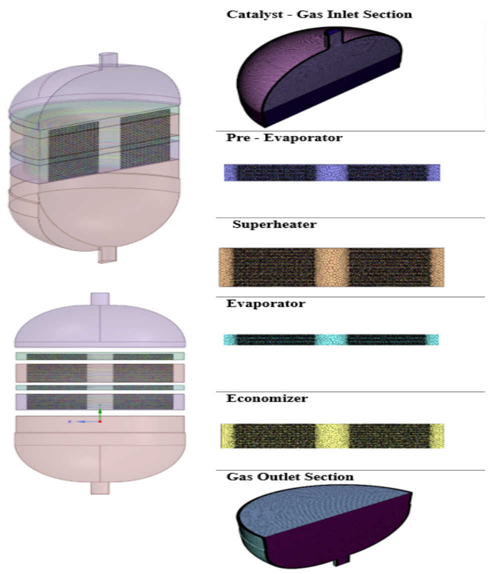

Figure 6. Model Mesh Structure of Ammonia Oxidation Reactor (AOR) Sections

The study used an Ansys Watertight Geometry mesh module to generate a mesh in the reactor inlet and catalyst section. Infiltration was defined on the system walls, and the total number of elements was determined to be 1755000. In the mesh thrown into section 1. (catalyst - gas inlet section), orthogonal quality was 0.20. Since the value obtained in orthogonal quality is desired to be close to 1, a result between 0.15-0.20 is acceptable. The skewness value was found to be 0.799. Since this value is chosen to be close to 0, a value between 0.5-0.8 is a good result. The total number of elements for the 2nd section (pre - evaporator) is 4355000, the total number of elements for the 3rd section (superheater) is 7872000, the total number of elements for the 4th section (evaporator) is 4355000, the total number of elements for the 5th section (economizer region) is 6600000, and the total number of elements for the 6th section outlet region is 2120000. The mesh independence graph obtained against the number of elements and created based on temperature and pressure values is also shown in Figure 7.

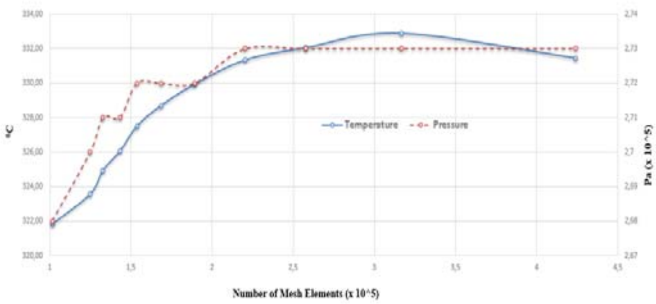

Figure 7. Grid Independence

The solver type in ANSYS Fluent is determined to be pressure-based and in a steady state (Kishan et al., 2020). Realizable SST k-omega is selected as the turbulent flow model. In addition, the effects of pressure gradient and buoyancy forces are also taken into account. The convergence criterion is 1E-06 for continuity and 1E-04 for other parameters. For analyses with Ansys Fluent, simulations were performed using the settings and conservation equations in Table 2.

Table 2. Settings and conservation equations used for CFD Simulations

Energy	On
Species Model	Species Transport Model-Mixture Material
Viscous Model	K-omega (2 equations)
K-omega Model	SST
Options	-Low-Re Correction
	-Viscous Heating
	-Curvature Correction
	-Production Limiter
	-Buoyancy Effect (Full)
General	-Steady State
	-Gravity (on)
Metarial	H_2O 16,35 %
	N_2 68,25 %
	NO 9,8 %
	O_2 5,6 %

In ANSYS Fluent, the upper reactor inlet is defined as a "velocity inlet." The lower reactor outlet is defined as a "pressure outlet." The serpentines in the waste heat boiler section of the ammonia oxidation reactor are spiral-shaped. They are wrapped from the inside out as a sleeve pie. The serpentines are arranged in a way that they are 29 layers on top of each other and connected. Since the NO_x gas flowing through the reactor's main body and the water flow passing through the coils are turbulent, the Realizable k-ω turbulence model was chosen as the turbulence model to get closer results. With a parametric study, the flow and hydrodynamic structure (velocity, temperature, and pressure distributions) of NO_x gas coming from the regions where the economizer, evaporator, superheater, and pre-evaporator coils are located were examined with the help of CFD analysis. The boundary conditions, gas properties, and material properties used for Ansys Fluent Analysis are also shown in Table 3.

Table 3. Input Gas Operating Values (Boundary Conditions) and Material Properties of the Reactor

Operating Values of Inlet Gas		Material Properties of the Reactor	
Inlet Pressure	342.000 Pa	Superheater	13 CrMo4-5
Input Velocity	29 m/s	Vaporizer	P235GH
Input Flow Rate	51.525 Nm^3/h	Pre-Evaporator	P235GH
Inlet Temperature	870 °C	Economizer	SA213

The plant SCADA gas pressure values comparison with CFD model values (with error percentages) is shown in Figure 8, and the plant SCADA gas velocity values comparison with CFD model values (with error percentages) is also shown in Figure 9. This online SCADA data from the plant (such as gas pressure and velocity values) provides us with real-time measurements of plant operations. Since the CFD model data is compatible with this data, the model is proven to be accurate and reliable. A validated model also more reliably predicts how design improvements will work.

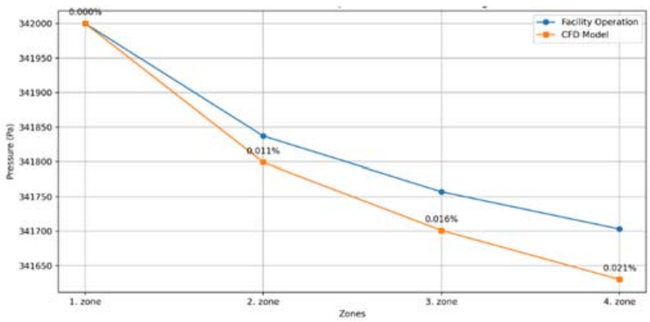

Figure 8. Comparison of Facility SCADA Gas Pressure Values with CFD Model Values (with error percentages)

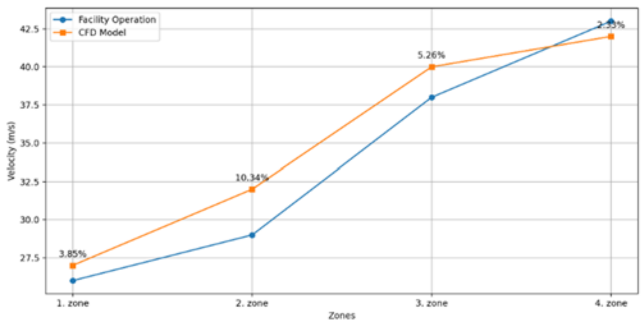

Figure 9. Comparison of Facility SCADA Gas Velocity Values with CFD Model Values (with error percentages)

Table 4. gives the numerical values used for the parametric study in the reactor analysis with the CFD model. In this study, for parametric study with CFD analysis, four parameter values were examined separately; these models:

1. Analysis model: The horizontal distance value (a) between the heat exchanger pipes was studied. In the current operation, the horizontal distance value between the heat exchanger pipes of the reactor is (a) = 48 mm. Parameter values of 44 mm, 46 mm, 52 mm, and 54 mm were created to find the optimum level for the horizontal distance between heat exchanger pipes.

Table 4. Numerical Values Used for Parametric Study in the Analysis of the Reactor with CFD Model

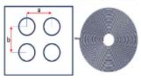			
Between Pipes Horizontal Distance (a)	**Between Pipes Vertical Distance (b)**	**Between Heat Exchanger Packages Distance (L)**	**Pipe Diameter (D)**
Current Reactor (48mm)	Current Reactor (63mm)	Current Reactor (0mm)	Current Reactor (42mm)
44 mm	57 mm	100 mm	38 mm
46 mm	60 mm	150 mm	40 mm
52 mm	66 mm	250 mm	44 mm
56 mm	69 mm	300 mm	46 mm

2. Analysis model: The vertical distance value (b) between the heat exchanger pipes was studied. In the current operation, the perpendicular distance between the heat exchanger pipes of the reactor is (b) = 63 mm. Parameter values of 57 mm, 60 mm, 66 mm, and 69 mm were created to find the optimum level for the vertical distance between heat exchanger pipes.

3. Analysis model: The distance (L) between heat exchanger packages (pre-evaporator, superheater, evaporator, and economizer) was studied. In the current operation, the distance between the heat exchangers in the reactor is (L) = 0 mm. So it is all on top of each other. To find the optimum exchanger arrangement, parameters of 100 mm, 150 mm, 250 mm, and 350 mm were created.

4. Analysis model: The heat exchangers' pipe diameter (D) was studied. Currently, the reactor's heat exchanger group pipe diameters are (D) = 42 mm. Parameter values of 38 mm, 40 mm, 44 mm, and 46 mm were created to find the optimum heat exchanger pipe diameter. While creating these parameters, the most efficient values were tried to be seen by comparing the values above and below them based on the existing operating data.

RESULTS AND DISCUSSION

The NH_3 boiler produces nitrous gases and recovers the heat produced during the reaction. Ammonia enriched with O_2 undergoes catalytic combustion (oxidation) at the Pt-Rh gauze in each reactor. Before starting the catalytic reaction, the platinum gauze in the catalyst basket is heated by a stationary H_2 ignitor. The process begins with the ignition of H_2, which initiates the oxidation of ammonia (NH_3) with compressed air, leading to catalytic combustion (Pottbacker et al., 2022; Kayapinar et al., 2024). The reaction is exothermic, and the combustion temperature can be controlled by adjusting the ratio of ammonia and air.

The nitrous gases are cooled downstream of the catalyst gauze using heating surfaces. Heat is transferred to water in the pre-evaporator, superheater, evaporator, and economizer to cool the NO_x process gas formed in the catalyst due to oxidation in the system. An instant SCADA image of the ammonia oxidation reactor during operation is shown in Figure 10. The feed water is heated in the economizer located in the process gas cooler. This heated water then flows into the steam drum, compensating for the water partly evaporated in the evaporator heating surfaces in the PGC. Circulation pumps provide the boiler water circulation. The steam drum separates the water-steam mixture, and the saturated steam is superheated in the superheater. An attemperator is located in the water volume of the steam drum, where a part of the superheated steam flow is cooled down to control the required superheated steam temperature.

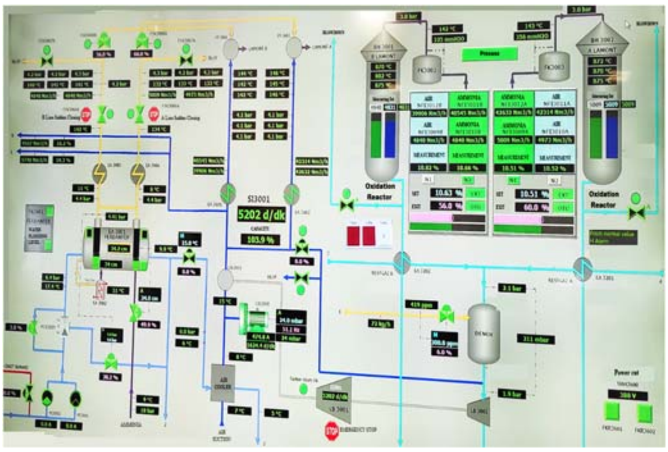

Figure 10. Instant SCADA View of Oxidation Reactors

Steam and water side of the process operating data and gas analysis values in the catalyst basket Table 5. is also given.

Table 5. Analysis Content of The Gas in The Catalyst Basket and Operating Values of the Steam-Water Side

Operating Data For Steam and Water Side		Gas Analysis at Catalyst Basket	
Parameter	**Value**	**Parameter**	**Vol %**
Steam generation (at 100% state)	36500 kg/h	H_2O	16,35
Blowdown (maximum)	1-2 %	N_2	68,25
Steam temperature	430 ^{0}C	NO	9,8
Steam pressure	41 barg	O_2	5,6
Feed water temperature	150 °C	Design pressure, gas side 4,5 barg	

The primary function of cooling devices in an ammonia oxidation reactor is to manage the temperature of the gases leaving the reactor. Figure 11. shows the process of gas entry-exit points to the pre-evaporator tube packages, symmetrical plane details, and the temperature distribution of the fluid in the heat exchanger tubes.

By cooling these hot process gases and promoting the evaporation of water flowing through the system, these devices effectively dissipate excess heat and prevent overheating within the reactor system. Effectively cooling hot process gases and promoting water evaporation, this application zone plays a critical role in maintaining desired temperature conditions in the ammonia oxidation reactor. This helps ensure efficient and safe reactor operation while minimizing the risk of thermal problems or equipment damage.

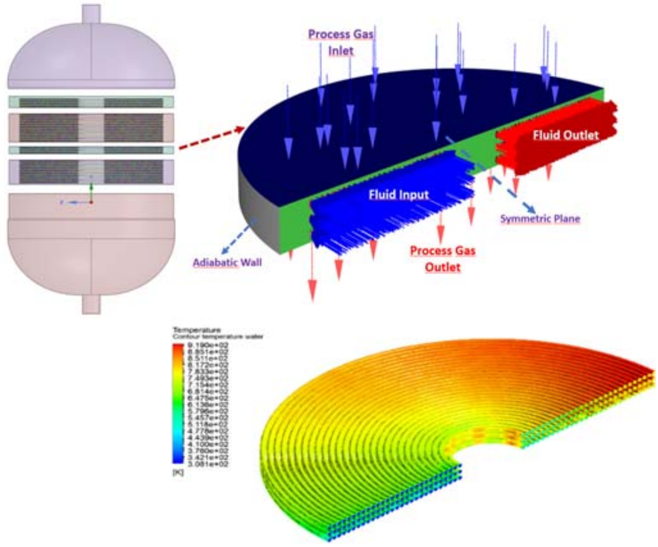

Figure 11. Temperature Distribution for Fluid Input-Outlet Points and Water Side of Pre-Evaporator Tube Packages Analyzed with CFD

The temperature distribution contours formed on the inlet and outlet for the gas side of the pre-evaporator in the ammonia oxidation reactor are shown below (Figure 12).

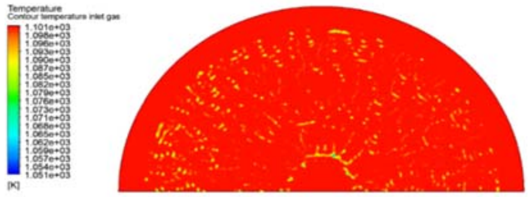

(a) Process Gas Inlet

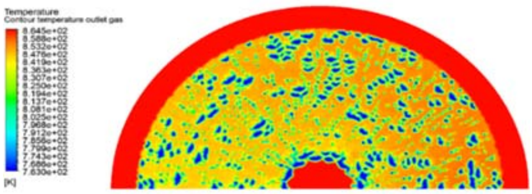

(b) Process Gas Outlet

Figure 12. Temperature Distribution Contours of the Process Gas Inlet (a) and Outlet (b) in the Pre-evaporator

Effect of Distance Between Heat Exchanger Packages on Gas Cooling

The heating surfaces consist of tube coils, parallel arranged in a spiral. One spiral is one layer located among each other and vertically oriented to the gas flow in the vessel. The spiral heating surfaces are surrounded by wall cooling coils, protecting the vessel shell. The feed water is heated in the economizer before entering the steam drum. The economizer heating surface consists of 10 layers. The ten layers are fed by 20 inlets and routed in a 2-way cross-flow.

The distributor and collector are arranged externally on the vessel. The saturated steam is superheated in the superheater. The superheater surface is made of parallel arranged tube banks horizontally in layers. There are always two layers connected. Figure 13. shows the CFD model results of the oxidation reactor analyzed with 100, 150, 250, and 300 mm gaps between the heat exchanger packages. The temperature values at the system outlet were measured as 329.73, 327.12, 326.685, and 323.205°C, respectively.

The minimal differences between the outlet temperatures indicate that the distance between the exchangers minimizes thermal performance. It is also seen that the velocity and pressure values at the system outlet are pretty close to each other. The results obtained show that the effects depending on the distance are limited. If the distance does not create an impact that will change the temperature or velocity profiles of the fluid, its effect on thermal performance is also minimal.

In the reactor currently in operation, the heat exchanger tube packages (pre-evaporator, superheater, evaporator, and economizer) used to cool the process gas were designed without leaving any space between them. The CFD study compared and analyzed the models created with 100, 150, 250, and 300 mm distances between these heat exchanger packages.

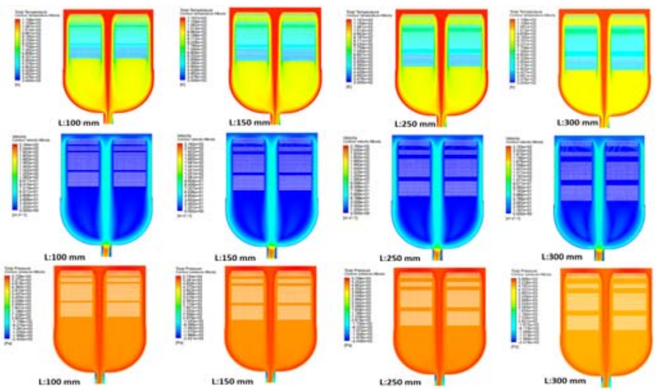

Figure 13. Effect of Distance Between Heat Exchanger Packages on Temperature, Speed, and Pressure (CFD Model Results)

Proper spacing and routing help maintain an even temperature throughout the gas flow, preventing hot spots or areas of inadequate cooling. Increasing the performance in heat exchanger tube packages will also mean increasing performance in the gas cooling process.

The optimum distance between tube packages will increase the heat transfer rate. It is necessary to have the proper amount and quality of feed water, heating steam, and cooling water. It should be done slowly when hot water fills to avoid thermal stress or shock on the pumps.

In Figure 14, the effect of the distance between heat exchanger packages on the temperature and pressure of the cooling process gas is shown by comparing all models. Sufficient optimum space between packages makes inspection, cleaning, and repair activities easier. Conversely, tight intervals can create difficulties for maintenance personnel and increase downtime during service.

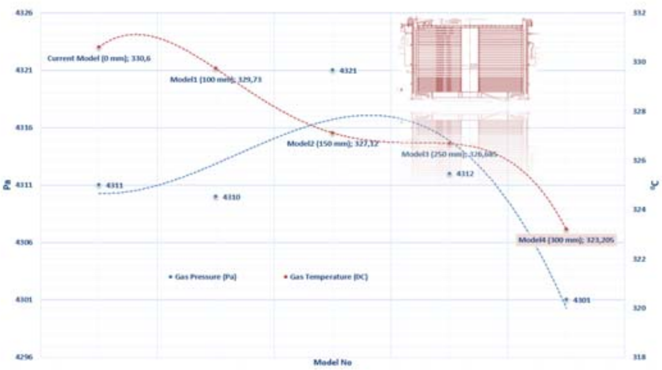

Figure 14. Effect of Distance Between Heat Exchanger Packages (HEP) Cooling Process Gas on Temperature and Pressure

Effect of Horizontal and Vertical Distance Between Heat Exchanger Tubes on Gas Cooling

The distance between heat exchanger tubes is critical in gas cooling systems, affecting heat transfer efficiency, temperature distribution, pressure drop, system optimization, maintenance, and overall economy. For a given number of pipes, the smaller the pipe spacing, the smaller the body diameter and, therefore, the lower the cost. As a result, designers tend to bundle together as many pipes as mechanically possible. However, in the case of heat transfer (thermal-hydraulic or thermo-hydraulic), the optimum pipe spacing and pipe diameter ratio must be determined to convert pressure into heat transfer. Closer spacing will result in insufficient fluid permeability by the body-side fluid and difficulty in mechanically cleaning the outer surfaces of the tubes.

The gap between the heat exchanger tubes can affect the temperature distribution of the gas as it passes through the cooling system. Proper spacing ensures even cooling throughout the gas flow, preventing hot spots or undercooled areas. A smaller distance may lead to less pressure drop and increase the risk of flow instability. Widening the horizontal distance between heat exchanger pipes ensures homogeneous fluid distribution (Noorollahi et al., 2018). This provides a more equal heat transfer and a more homogeneous temperature distribution. The narrowing of the horizontal distance between pipes causes the flow to accelerate and local flow velocities to increase. In this case, the temperature profile is irregular, and heat transfer is less in certain regions.

Figure 15. shows the effect of the horizontal distance between the heat exchanger tubes on temperature, speed, and pressure (CFD model results). The outlet temperature was measured as 334.95 °C when the horizontal distance between the tubes was 44 mm, 327.12 °C when the distance between the tubes was 46 mm, 286.23 °C when the distance between the tubes was 52 mm, and 270.51°C when the distance between the tubes was 56 mm. When the distance between the tubes was increased, the resistance to flow decreased, and the thermal efficiency increased because, especially by improving the horizontal distance between the tubes and reducing the cross-sectional area of the fluid passing through the middle of the system, a homogeneous pipe distribution was obtained in the system. Increasing the distance between the tubes ensures that the fluid encounters fewer obstacles throughout the exchanger. This reduces the flow resistance and optimizes turbulence at the same time.

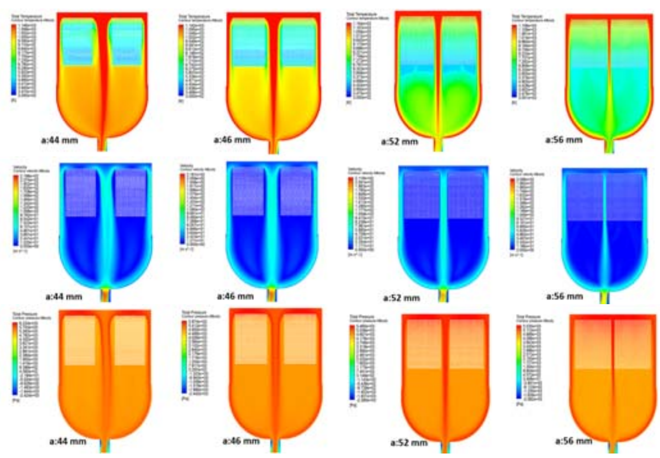

Figure 15. Effect of Horizontal Distance Between Heat Exchanger Pipes on Temperature, Speed, and Pressure (CFD Model Results)

Figure 16. shows the effect of the horizontal distance between the heat exchanger pipes on the temperature and pressure of the cooling process gas. Regarding facility and system efficiency, the lowest temperature of the process gas (270.51⁰C) was obtained in the model with a horizontal distance of 56 mm. This was the best cooling performance model obtained among all parametric study models.

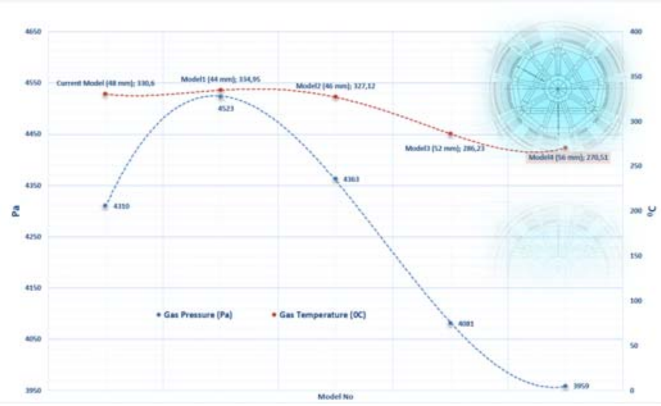

Figure 16. Effect of Horizontal Distance Between Heat Exchanger Pipes on Temperature and Pressure of Cooling Process Gas

The vertical distance between the heat exchanger pipes in the gas cooling zone of the existing oxidation reactor is 63 mm. Figure 17. the CFD model results of the oxidation reactor were analyzed with a vertical distance of 57, 60, 66, and 69 mm between the heat exchanger pipes. As a result of the studies, when the perpendicular distance between the pipes is 57 mm, the system outlet temperature is measured as 318.42 °C; for 60 mm, it is 319.29 °C; for 66 mm, it is 320.59 °C, and for 69 mm, it is 321.9 °C. As seen in Figure 9, where the effect of the distance between the exchangers on the system efficiency is examined, it has been determined that its impact is low. In addition, it has been observed that thermal efficiency decreases when the distance between the pipes increases vertically.

In this case, it has been determined that the most efficient model has a vertical distance of 57 mm. Increasing the vertical distance reduces the pipe density in the exchanger.
A less dense pipe arrangement causes the gas fluid to pass more efficiently throughout the system without losing energy. However, this also causes the fluid to leave the system without cooling sufficiently, which increases the outlet temperature. It also causes the thermal interaction areas around each pipe to decrease.

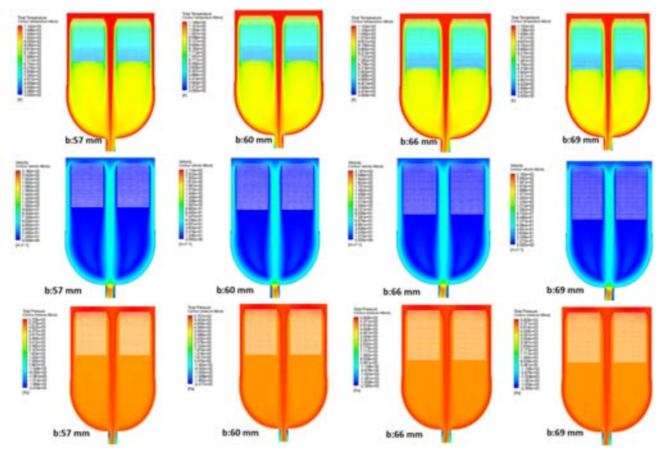

Figure 17. Effect of Vertical Distance Between Heat Exchanger Pipes on Temperature, Speed, and Pressure (CFD Model Results)

This results in the "heat transfer effect" created by the pipes on the fluid becoming isolated from each other. Thus, the synergistic heat transfer between the pipes is reduced. Since the fluid spends less time between the pipes, the heat exchange with the pipes is also restricted. This causes the gas to leave the system at a higher temperature. Figure 18. shows the effect of the vertical distance between the heat exchanger pipes on the temperature and pressure of the cooling process gas. Regarding facility and system efficiency, the lowest temperature of the process gas (318 ⁰C) was obtained in the model with a vertical distance of 57 mm.

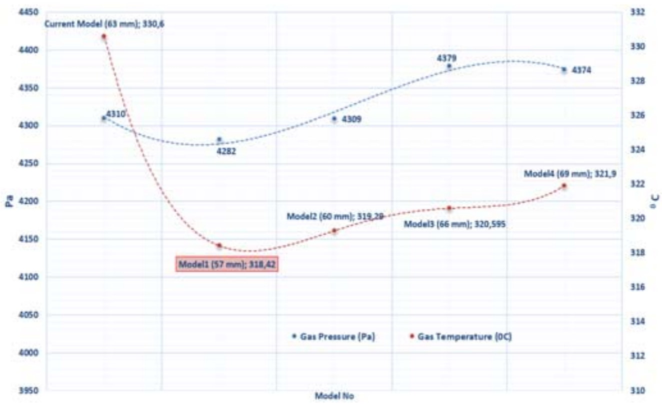

Figure 18. Effect of Vertical Distance Between Heat Exchanger Pipes on Temperature and Pressure of Cooling Process Gas

Effect of Heat Exchanger Tube Diameter on Gas Cooling

The heat exchanger pipe diameters in the existing oxidation reactor gas cooling zone are 42 mm. Figure 19. the CFD model results of the oxidation reactor were analyzed with heat exchanger pipe diameters of 38, 40, 44, and 46 mm. When the temperature contour graphs are examined, the system outlet temperature for the diameter of 38 mm is measured as 296.67 °C, for 40 mm as 310.15°C, for 44 mm as 325.38 mm, and for the diameter of 46 mm as 334.51°C. It has been determined that the change in diameter significantly affects the system efficiency and that the most efficient model is a diameter of 38 mm. Since this diameter value offers a higher surface area-to-volume ratio compared to the others, the heat transfer efficiency increases. As the diameter increases, the gas cooling performance decreases. It can be said that small-diameter pipes increase the total heat transfer surface by fitting more pipes in the same area.

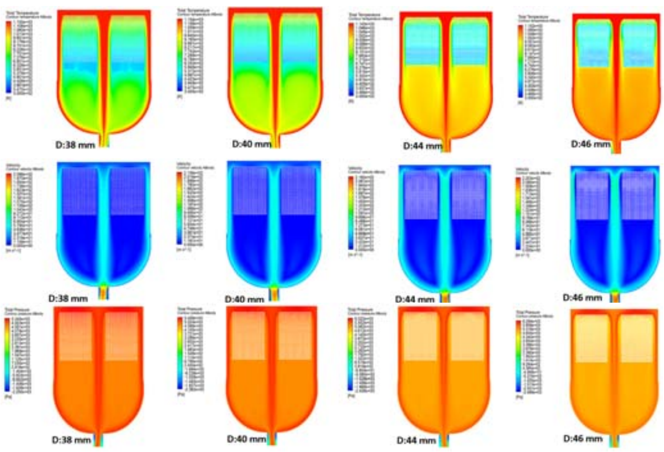

Figure 19. Effect of Heat Exchanger Pipe Diameter on Temperature, Speed, and Pressure (CFD Model Results)

The effect of heat exchanger pipe diameter on cooling process gas temperature and pressure is shown in Figure 20. Many parameters are effective in the optimization and design of heat exchangers. The manufacturing method of the heat exchanger, the heat transfer mechanism, and the flow states of the fluids are effective in the design and efficient use of heat exchangers. Regarding facility and system efficiency, the lowest temperature of the process gas (296.67 ^{0}C) was obtained in the model with a pipe diameter of 38 mm. In the process of cooling the process gas, the hot gas fluid that comes into contact with the surface area of the heat exchanger tube packages at low speeds provides a better performance with smaller diameter heat exchanger pipes (with water circulating in them).

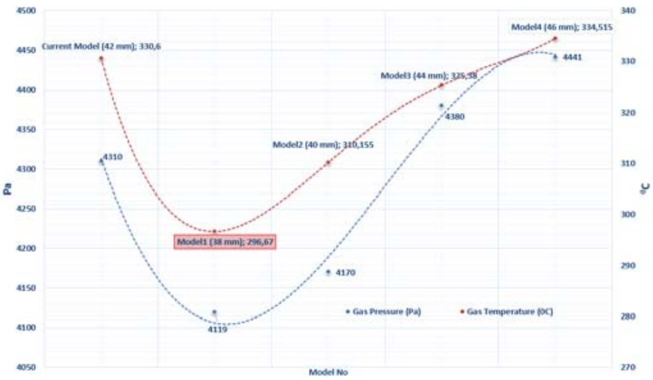

Figure 20. Effect of Heat Exchanger Pipe Diameter on Cooling Process Gas Temperature and Pressure

Because it ensures that the fluid (water) remains in the pipes for longer, providing more heat transfer. Additionally, smaller diameter pipes offer a more compact design. Thus, providing a better flow distribution and a more homogeneous temperature profile increases efficiency by delivering more heat transfer surfaces. An important point to consider while cooling the process gas is this: during regular operation, the circulation water is circulated by electrically driven pumps. Flow measurements are taken and monitored for accurate control. Additionally, a second electrically-driven pump is available as a standby in case of any issues. Low water-steam mixture velocities can cause water-steam separation in the horizontally designed evaporator heating surfaces. This can decrease the cooling efficiency of the upper part of the tubes, leading to overheating and severe damage. Using smaller diameter pipes in the liquid passing parts on the cold side has been observed to affect several factors that increase heat transfer. When the pipe diameter decreases for the same flow rate, the flow rate increases, which makes the flow more dynamic. Increasing velocity causes the liquid to interact more with the pipe wall, increasing heat transfer. In smaller-diameter pipes, the possibility of the flow becoming turbulent increases. Turbulent flow increases heat transfer coefficients because the movement of the fluid provides better mixing and temperature distribution. These factors explain why the pipes through which the liquid on the cold side passes are smaller in diameter, increasing heat transfer and, therefore, cooling performance. However, these advantages may vary depending on the overall design of the system and operating conditions.

Table 6. gives the hourly SCADA data (process gas temperature and flow rate values) taken online at operating conditions for the ammonia oxidation reactor of the relevant nitric acid production facility. Additionally, Table 7 compares this study's design values with those obtained in studies in the literature. When the actual operating SCADA values of the ammonia oxidation reactor modeled with CFD analysis are examined, it is seen that the gas outlet temperature is around 297 ^{0}C on average. Considering this average temperature value, a decrease in gas temperature of approximately 9% was achieved with this study.

Table 6. Hourly SCADA Data for Process Gas Temperature and Flow Rate in Ammonia Oxidation Reactor

Time	Process gas inlet (^{o}C)	Process gas outlet (^{o}C)	Process gas flow (Nm^3/h)
02:00	870	297	51700
04:00	874	296	52100
06:00	874	298	52374
08:00	879	297	51680
10:00	870	297	51630
12:00	877	299	51706
14:00	871	296	51620
16:00	874	298	51600
18:00	875	299	51843
20:00	881	293	52495
22:00	866	292	52444
00:00	871	296	52470

When the absolute operating SCADA values of the ammonia oxidation reactor modeled with CFD analysis are examined, it is seen that the gas outlet temperature is around 297 ^{0}C on average. Considering this average temperature value, a decrease of approximately 9% in gas temperature has been achieved with this study.

Table 7. Comparison of Values for Different Models in the Ammonium Oxidation Reactor

Model	Reactor Zone	System Conditions
This study	Heat exchangers	Average gas flow: 51971 Nm^3/h Reactor Height: 6500 mm Gas side pressure:4.5 barg
Abbasfard et al., (2012)	Reactor inlet and distributor	Gas inlet speed: 13.77 m/s Outlet pressure: 5.33 bar Nominal flow: 32543 m^3 / h
Grande et al. (2018).	Platinum catalyst	Activation energy: 114 kJ/mol Pressure value: 4.7 bar Flow rate value: 1.698 SLPM
Amirsadat et al. (2024)	Inlet feed pipeline	Pressure value: 12.65 bar Nominal flow: 6466 m^3 / h Reactor Height: 9082 mm
Nascimento et al. (2024).	Absorption column	Pressure value: 456.62 kPa Air molar flow: 310.74 kmol/h Cooling coils area: 8.47 m^2

This decrease in the percentage of cooling of these hot NOx gases formed due to chemical reactions in the ammonia oxidation reactor catalyst is significant for the following criteria and system reactions. Because as the temperature value decreases,

- NOx gases (especially NO and NO_2) have high energy and tend to enter side reactions.
- The chemical stability of NO_x gases increases; this prevents undesirable reactions.
- This gas leaving the reactor is then sent to the absorption towers. As the gas temperature decreases, the reaction kinetics accelerates due to the low solubility of the gases. The conversion rate of NO_x to nitric acid and product efficiency also increases.

The distribution of maximum temperature values for steam is necessary to manage major critical factors such as equipment life, energy exchange, chemical change, system stability, and observed protection. High temperatures can cause metal surfaces to melt, oxidize, or expand, leading to equipment failure. These temperature limitations help the system to be efficient, safe, and long-lasting.

Extreme temperatures can create extreme stresses on valves, pipelines, and other components in the system. Based on the design of the heat exchanger packages of the ammonia oxidation reactor of the relevant facility, the maximum fluid (water) temperature was limited to 266 ^{0}C in the economizer and evaporator and 470^{0}C in the superheater. With CFD simulation analysis, the model results in which the lowest process gas temperature was obtained with a 56 mm horizontal distance between the heat exchanger pipes were compared with the actual operating values obtained from the facility's online SCADA data system.

Accordingly, there was an increase of 8.2% in the fluid outlet temperature obtained in the economizer, 9.7 % in the evaporator, and 4.3 % in the superheater. These changes received as a result of the simulation are consistent with the temperature values that are the basis for the design and the limited ones. Table 8. shows the temperature change values of the fluid circulating in the heat exchanger packages.

Table 8. Temperature change values of the fluid in the heat exchanger packages

Component	a	b	c
Facility SCADA Data System Fluid Temperature (^{0}C)	430	301	202
CFD Simulation Data Fluid Temperature (^{0}C)	448,4	330.1	218,5
Rate of Increase in Temperature Value (%)	4.3	9.7	8.2

a: Superheater b: Evaporator c: Economizer

Other problems affecting the gas cooling process and solution suggestions

After a shutdown or emergency stop of the process gas cooler, the entire system must be vented after an ammonia trip to remove corrosive flue gas. If the gas cooler is disconnected from the steam network, the start-up valve must be activated to release the steam and cool the superheater. During this process, monitoring the outlet temperature at the superheater is crucial. Monitoring the overall circulation volume and current consumption during operation is essential to avoid overloading the circulation pump. As the heat-up process progresses, the circulation volume should be reduced at the discharge slide gate valve. The heat-up process commences by opening the steam injection valve to the steam drum. To control the heat-up process, the steam quantity and heat supplied and the steam discharge via the start-up valve should be adjusted. Ensuring a continuous steam flow to the drum is crucial to prevent hammering. During the heating-up process, it is essential to maintain the drum water level above the "low" level. The water level will increase due to thermal expansion and condensed heating steam. After the heating-up process commences, the water level should not decrease. Boiling out is a commonly used method for cleaning the water and water/steam system, involving fast temperature changes instead of chemicals. This method effectively dissolves iron oxide layers, dust, and sand while forming a protective magnetite layer (only above 200°C). Flushing is often done before boiling out. There are two methods for boiling out the Process gas cooler system: constant pressure and fluctuating pressure (respiratory method). The respiratory method is preferred as it accelerates flaking. Boiling out is most effective for new plants, while pickling is more efficient for existing plants where deposits have already formed in the pipes. The temperature can be monitored and controlled if there is a measurement in the water circulation system. When the drum pressure is 0.2 MPag, the valve should be closed. Once the steam pressure reaches around 0.2-0.3 MPag, the bypass valve of the steam traps can be closed, and the steam traps can be put into operation. During the heat-up phase and after the start of the reaction, the superheater and the superheated steam line must be drained repeatedly via the bypass valves. It is important to gradually increase the temperature of superheated steam, particularly during the initial heat-up phase, after ignition, and the start of catalytic combustion (when the attemperator is fully open). While heating up and after the reaction has started, it is necessary to repeatedly drain the superheated steam line and the superheaters via the bypass valves. The facility is heated up using external steam from the "20 atu net", which is nozzle-fed into the steam drum via a bleed pipe. To avoid water hammer, the steam valves must be opened slowly and carefully. During the heat-up, the water level of the drum must be within the visible range. It is not allowed to operate the system with a water level below "low."The manual regulating valve on the heating line adjusts the jet-fed external steam quantity. Steam hammering is to be avoided.

CONCLUSION

Proper gas flow and distribution within ammonia oxidation reactors are essential for a homogeneous reaction environment. A well-designed reactor system can achieve the desired conversion efficiency and ensure the process is economically and environmentally sustainable. One of the most critical parameters here is the NO outlet temperature. This NO gas formed in the catalyst reaches high temperatures until it enters the cooling exchangers. The system efficiency value decreases at every ^{o}C level where the NO outlet temperature exceeds the design value. The same model of the ammonia oxidation reactor of the 610 ton/day nitric acid production plant considered in this study was analyzed in CFD simulation. Regarding plant and system efficiency, the lowest temperature of the process gas (270.51°C) was obtained in the model where the horizontal distance between the heat exchanger tubes was 56 mm. The increased horizontal distance between the tubes allowed each tube to contribute equally to heat transfer and reduced the "dead zones" (where temperature changes are minimal). This model has shown the most effective cooling performance among all parametric study models. In response to the cooling performance of this hot gas, there has also been an increase in the current temperature values of the refrigerant circulating in the exchanger packages. When the CFD simulation results are compared with the actual operating data (SCADA online data), the fluid outlet temperature in the ammonia oxidation reactor has increased by 8.2% in the economizer, 9.7% in the evaporator, and 4.3% in the superheater. In other simulations, it has been observed that the distance between the exchanger packages has a minimal effect on the thermal performance (the speed and pressure values at the system outlet are pretty close to each other) and that the thermal efficiency decreases when the distance between the tubes is increased vertically and the tube diameter increases. Increasing the vertical distance between the tubes reduces the contact time to the heat transfer surface and the thermal interaction zones between the tubes. This results in lower thermal efficiency and higher outlet temperatures for hot gas cooling. The approximate temperature change for a vertical distance change of 12 mm is 3.48 °C. Therefore, vertical distance changes appear to have less impact on system efficiency. The following study aims to investigate the effect of different design types of La Mont nozzles, which are located at the inlet of each evaporator and wall cooling pipe, on the system efficiency (by CFD simulation analysis), ensuring that the required water flow reaches separate regions and that all sections are sufficiently cooled.

REFERENCES

Abbasfard, H., Ghanbari, M., Ghasemi, A., Ghader, S., Rafsanjani, H. H., & Moradi, A. (2012). Failure analysis and modeling of superheater tubes of a waste heat boiler thermally coupled in an ammonia oxidation reactor. *Engineering Failure Analysis*, *26*, 285-292. https://doi.org/10.1016/j.engfailanal.2012.06.012

Abbasfard, H., Ghanbari, M., Ghasemi, A., Ghahraman, G., Jokar, S. M., & Rahimpour, M. R. (2014). CFD modeling of flow maldistribution in an industrial ammonia oxidation reactor: A case study. *Applied thermal engineering*, *67*(1-2), 223-229. https://doi.org/10.1016/j.applthermaleng.2014.03.035

Amirsadat, S. M., Azari, A., Nazari, M., & Akrami, M. (2024). Conversion augmentation of an industrial NH3 oxidation reactor by geometry modification to improve the flow and temperature pattern uniformity using CFD modeling. *Chemical Engineering Journal Advances*, *19*, 100629. https://doi.org/10.1016/j.ceja.2024.100629

Ardy, H., Putra, Y. P., Anggoro, A. D., & Wibowo, A. (2021). Failure analysis of primary waste heat boiler tube in ammonia plant. Heliyon, 7(2). https://doi.org/10.1016/j.heliyon.2021.e06151

Bagheri, H., Bagheri, S., Hashemipour, H., & Rahimpour, M. R. (2024). Modeling and optimization of ammonia reactor. In *Progresses in Ammonia: Science, Technology and Membranes* (pp. 173-204). Elsevier. https://doi.org/10.1016/B978-0-323-88516-4.00001-9

Belghaieb, J., Dkhil, O., Elhajbelgacem, A., Hajji, N., & Labidi, J. (2010). Energy optimization of a network of exchangers-reactors in a nitric acid production plant. Chemical Engineering, 21. https://doi.org/10.3303/CET1021046

Chatterjee, I. B., & Joshi, J. B. (2008). Modeling, simulation, and optimization: Mono pressure nitric acid process. Chemical Engineering Journal, 138(1-3), 556-577. https://doi.org/10.1016/j.cej.2007.07.064

Chernyshev, V. I., & Zjuzin, S. V. (2001). Improved start-up for the ammonia oxidation reaction. Platinum Metals Review, 45(1), 22-30.

Colak, A. B., & Arslan, O. (2024). Numerical analysis-based performance assessment of the small-scale organic Rankine cycle turbine design for residential applications. *Thermal Science and Engineering Progress*, *51*, 102626. https://doi.org/10.1016/j.tsep.2024.102626

Dong, Y., Zhang, D., Li, D., Jia, H., & Qin, W. (2023). Control of Ostwald ripening. *Science China Materials*, *66*(3), 1249-1255. https://doi.org/10.1007/s40843-022-2233-3

Elsayed, S., & Farag, H. A. (2023). Modelling of an Industrial Reactor for Ammonia Oxidation. *ERJ. Engineering Research Journal*, *46*(4), 451-456. https://doi.org/10.21608/erjm.2023.142966.1177

Enger, B. C., Auvray, X., Lødeng, R., Menon, M., Waller, D., & Rønning, M. (2018). Catalytic oxidation of NO to NO_2 for nitric acid production over a Pt/Al2O3 catalyst. *Applied Catalysis A: General*, *564*, 142-146. https://doi.org/10.1016/j.apcata.2018.07.019

Fajardo, J., Valle, H., & Buelvas, A. (2018). Avoidable and Unavoidable Exergetic Destruction Analysis of a Nitric Acid Production Plant. In ASME International Mechanical Engineering Congress and Exposition (Vol. 52088, p. V06BT08A009). American Society of Mechanical Engineers. https://doi.org/10.2298/TSCI120503181V

Fíla, V., & Bernauer, B. (1994). A mathematical model of a gauze reactor for the ammonia oxidation. *Collection of Czechoslovak chemical communications*, *59*(4), 855-874. https://doi.org/10.1135/cccc19940855

García-Ruiz, P., Uruén, M., Abián, M., & Alzueta, M. U. (2023). High pressure ammonia oxidation in a flow reactor. *Fuel*, *348*, 128302. https://doi.org/10.1016/j.fuel.2023.128302

Grande, C. A., Andreassen, K. A., Cavka, J. H., Waller, D., Lorentsen, O. A., Øien, H., ... & Modeshia, D. (2018). Process intensification in nitric acid plants by catalytic oxidation of nitric oxide. *Industrial & Engineering Chemistry Research*, *57*(31), 10180-10186. https://doi.org/10.1021/acs.iecr.8b01483

Hannevold, L., Nilsen, O., Kjekshus, A., & Fjellvåg, H. (2005). Reconstruction of platinum–rhodium catalysts during oxidation of ammonia. *Applied Catalysis A: General*, *284*(1-2), 163-176. https://doi.org/10.1016/j.apcata.2005.01.033

Heck, R. M., Bonacci, J. C., Hatfield, W. R., & Hsiung, T. H. (1982). A new research pilot plant unit for ammonia oxidation processes and some gauze data comparisons for nitric acid process. *Industrial & Engineering Chemistry Process Design and Development*, *21*(1), 73-79. https://doi.org/10.1021/i200016a014

Hernández, A. B., Fajardo, J. G., Barreto, D., Caballero, G. E. C., Escorcia, Y. C., Tovar, C. R. V., & Hernández, Y. G. (2021). Conventional and advanced exergoeconomic indicators of a nitric acid production plant concerning the cooling temperature in compression Train's intermediate stages—case *Studies in Thermal Engineering*, *27*, 101214. https://doi.org/10.1016/j.csite.2021.101214

Holma, H., & Sohlo, J. (1979). A mathematical model of an absorption tower of nitrogen oxides in nitric acid production. *Computers & Chemical Engineering*, *3*(1-4), 135-141. https://doi.org/10.1016/0098-1354(79)80024-1

Hung, C. M. (2008). Catalytic wet oxidation of ammonia solution with platinum-palladium-rhodium composite oxide catalyst. *J. Environ. Eng. Manage*, *18*(2), 85-91.

Il'chenko, N. I., & Golodets, G. I. (1975). Catalytic oxidation of ammonia: II. Relationship between catalytic properties of substances and surface oxygen bond energy. General regularities in catalytic oxidation of ammonia and organic substances. Journal of Catalysis, 39(1), 73-86. https://doi.org/10.1016/0021-9517(75)90283-3

Juangsa, F. B., & Aziz, M. (2019). Integrated system of thermochemical cycle of ammonia, nitrogen production, and power generation. *International Journal of Hydrogen Energy*, *44*(33), 17525-17534. https://doi.org/10.1016/j.ijhydene.2019.05.110

Kayapinar, O., Arslan, A. E., Arslan, O., & Genc, M. S. (2024). Multi-criteria analysis on the simulation-based optimal design of a new stack-type natural ventilation system for industrial buildings. *Thermal Science and Engineering Progress*, *51*, 102657. https://doi.org/10.1016/j.tsep.2024.102657

Kirova-Yordanova, Z. (2011). Application of the exergy method to the environmental impact estimation: The nitric acid production as a case study. Energy, 36(6), 3733-3744. https://doi.org/10.1016/j.energy.2010.12.039

Kishan, R., Singh, D., & Sharma, A. K. (2020). CFD Analysis of heat exchanger models designs using Ansys fluent—International *Journal of Mechanical Engineering and Technology*, *11*(2). https://www.doi.org/10.34218/IJMET.11.2.2020.001

Kraehnert, R., & Baerns, M. (2008). Kinetics of ammonia oxidation over Pt foil studied in a micro-structured quartz-reactor. Chemical engineering journal, 137(2), 361-375. https://doi.org/10.1016/j.cej.2007.05.005

Lim, J., Fernández, C. A., Lee, S. W., & Hatzell, M. C. (2021). Ammonia and nitric acid demand for fertilizer use in 2050. *ACS Energy Letters*, *6*(10), 3676-3685. https://doi.org/10.1021/acsenergylett.1c01614

Mewada, R. K., & Nimkar, S. C. (2015). Minimization of exergy losses in mono high-pressure nitric acid process. International Journal of Exergy, 17(2), 192-218. https://doi.org/10.1504/IJEX.2015.069990

Moszowski, B., Wajman, T., Sobczak, K., Inger, M., & Wilk, M. (2019). The analysis of distribution of the reaction mixture in ammonia oxidation reactor. Polish Journal of Chemical Technology, 21(1), 9-12. https://doi.org/10.2478/pjct-2019-0002

Nascimento, G. R., & Dangelo, J. V. (2024). Operating parameters analysis of a nitric acid plant to increase production and reduce NOx gases emission. *Chemical Engineering and Processing-Process Intensification*, *196*, 109662. https://doi.org/10.1016/j.cep.2024.109662

Neumann, N. C., Baumstark, D., Martínez, P. L., Monnerie, N., & Roeb, M. (2024). Exploiting synergies between sustainable ammonia and nitric acid production: A techno-economic assessment. *Journal of Cleaner Production*, *438*, 140740. https://doi.org/10.1016/j.jclepro.2024.140740

Noorollahi, Y., Saeidi, R., Mohammadi, M., Amiri, A., & Hosseinzadeh, M. (2018). The effects of ground heat exchanger parameters changes on geothermal heat pump performance–A review. *Applied Thermal Engineering*, *129*, 1645-1658. https://doi.org/10.1016/j.applthermaleng.2017.10.111

Pfefferle, L. D., & Pfefferle, W. C. (1987). Catalysis in combustion. *Catalysis Reviews Science and Engineering*, *29*(2-3), 219-267. https://doi.org/10.1080/01614948708078071

Pottbacker, J., Jakobtorweihen, S., Behnecke, A. S., Abdullah, A., Özdemir, M., Warner, M., ... & Horn, R. (2022). Resolving gradients in an ammonia oxidation reactor under industrial conditions: A combined experimental and simulation study. *Chemical engineering journal*, *439*, 135350. https://doi.org/10.1016/j.cej.2022.135350

Process Gas Coolers Operation and Maintenance Manual (2024). Istanbul Fertilizer Industry Inc. Kutahya Production Facilities.

Rajeshkumar, M., Logesh, K., Thangaraj, M., & Govindan, S. (2021). Heat transfer study on finned tube heat exchanger using CFD. *International Journal of Ambient Energy*, *42*(3), 239-243 https://doi.org/10.1080/01430750.2018.1542621

Sadykov, V. A., Isupova, L. A., Zolotarskii, I. A., Bobrova, L. N., Noskov, A. S., Parmon, V. N., ... & Lunin, V. V. (2000). Oxide catalysts for ammonia oxidation in nitric acid production: properties and perspectives. *Applied Catalysis A: General*, *204*(1), 59-87. https://doi.org/10.1016/S0926-860X(00)00506-8

Salam, M. A., Nassef, E., Elkheriany, E., & El Tawel, Y. (2016). Modeling and Simulation of Gauze Reactor of Ammonia Oxidation. *American Journal of Chemical Engineering*, *4*(1), 16-22. https://doi.org/10.11648/j.ajche.20160401.13

Scheuer, A., Hirsch, O., Hayes, R., Vogel, H., & Votsmeier, M. (2011). Efficient simulation of an ammonia oxidation reactor using a solution mapping approach. *Catalysis Today*, *175*(1), 141-146. https://doi.org/10.1016/j.cattod.2011.03.036

Schumacher, K., Engelbrecht, N., Everson, R. C., Friedl, M., & Bessarabov, D. G. (2019). Steady-state and transient modelling of a microchannel reactor for coupled ammonia decomposition and oxidation. *International Journal of Hydrogen Energy*, *44*(13), 6415-6426. https://doi.org/10.1016/j.ijhydene.2019.01.132

Song, Y., Hashemi, H., Christensen, J. M., Zou, C., Marshall, P., & Glarborg, P. (2016). Ammonia oxidation at high pressure and intermediate temperatures. *Fuel*, *181*, 358-365. https://doi.org/10.1016/j.fuel.2016.04.100

Srinivasan, R., Hsing, I. M., Berger, P. E., Jensen, K. F., Firebaugh, S. L., Schmidt, M. A., ... & Ryley, J. F. (1997). Micromachined reactors for catalytic partial oxidation reactions. *AIChE Journal*, *43*(11), 3059-3069. https://doi.org/10.1016/j.ces.2007.09.021

Stagni, A., Cavallotti, C., Arunthanayothin, S., Song, Y., Herbinet, O., Battin-Leclerc, F., & Faravelli, T. (2020). An experimental, theoretical and kinetic-modeling study of the gas-phase oxidation of ammonia. *Reaction Chemistry & Engineering*, *5*(4), 696-711. https://doi.org/10.1039/C9RE00429G

Wiser, Artur M. (2020), Investigation of the Industrial NH3 Oxidation by CFD Simulations Including Detailed Surface Kinetics (Ph.D. thesis), Technische Universität Darmstadt. https://doi.org/10.25534/tuprints-00017208

Zhan, H., Li, S., Yin, G., Hu, E., & Huang, Z. (2024). Experimental and kinetic study of ammonia oxidation and NOx emissions at elevated pressures. *Combustion and Flame*, *263*, 113129. https://doi.org/10.1016/j.ijhydene.2024.12.214